J. Water Environ. Nanotechnol., 7(4): 344-350 Autumn 2022

ORIGINAL RESEARCH PAPER

Synthesis and characterization of Sn-doped TiO_2 nanoparticles and the evaluation of their Photocatalytic performance under Vis-lights

Hassanali Rasouli[1], Faezeh Jafarpisheh[2], Mohammad Ghorbanpour[2,*]

[1] Faculty of Engineering, University of Mohaghegh Ardabili, Ardabil, Iran
[2] Chemical Engineering Department, University of Tabriz, Tabriz, Iran

Received: 2022-07-16 Accepted: 2022-09-07 Published: 2022-10-01

ABSTRACT

Dyes are produced as water pollutants in the textile, plastic, and dye industries. Many efforts have been made to remove dyes from industrial wastewater. In this area, Photocatalytic performance under Vis-lights is a useful and effective method. In this study, a series of highly efficient Sn-doped TiO_2 photocatalysts were successfully developed using a simple heat treatment process. Three concentrations of $SnCl_2$ powder (3%, 5%, and 7 %) were used for the preparation of materials. The characterizations of resulting materials were distinguished by scanning electron microscopy (SEM), diffusion reflection spectroscopy (DRS), and X-ray diffraction spectroscopy (EDX). Also, methyl orange dye was served to indicate the photocatalytic activity of Sn-doped material under visible light irradiation. The results indicated that both doped and also pure TiO2 have a uniform size. Anatase was the only identified phase in all the products, whether doped or un-doped. The resulting Sn-doped materials have demonstrated a band gap value range of 3.14 to 2.68 eV in comparison with pure TiO_2 which shows a value of 3.2 eV. The photocatalytic evaluations indicated that the samples prepared in the presence of 3, 5, and 7% $SnCl_2$ have degradation efficiencies of 85%, 85%, and 90%, respectively within 120 min, which are much higher than that of un-doped TiO_2. The enhancement in the efficiency was attributed to the gap changes in anatase by the incorporation of Sn ions into the TiO_2 lattice structure. Compared to pure TiO_2, which has a band gap of 3.2 eV, the band gap values for doped TiO_2 ranged from 3.14 to 2.68 eV.

Keywords: *Photocatalyst, Sn-doped TiO_2, Nanoparticles, Anatase.*

How to cite this article
Rasouli H., Jafarpisheh F., Ghorbanpour M. Synthesis and characterization of Sn-doped TiO_2 nanoparticles and the evaluation of their Photocatalytic performance under Vis-lights. J. Water Environ. Nanotechnol., 2022; 7(4): 344-350.
DOI: 10.22090/jwent.2022.04.001

INTRODUCTION

Titanium dioxide nanoparticles are known to be predominant semiconductors [1]. Production of sensors [2], biocide agents [3,4], hydrogen [5], photo-catalysts [6,7], and water evaporation reduction [8] are just a few of the applications of TiO_2. These particles are non-toxic, chemically stable, low-cost, and also have good optical qualities. When TiO_2 nanoparticles are excited under light irradiations, they can hydrolyze organic molecules in an aqueous solution. Absorption of light which has an energy equal to or greater than the band gap (3.2 eV) causes the excitation of electrons from the valence band to the conduction band of the semiconductor [9]. Hydroxyl radicals, which are powerful oxidants of organic molecules, are formed as a result of this. Unfortunately, considering that titanium dioxide has a large band gap energy (3.2 eV), it can only be excited by absorbing UV light. As a result, many researchers have aimed to improve TiO_2's photocatalytic effectiveness under visible light, regarding that the light produced by the sun is significantly far better accessible than UV

* Corresponding Author Email: *Ghorbanpour@uma.ac.ir*

[10]. Doping the aforementioned semiconductor with metals such as Cu [11], Sn [12,13], Fe [14], Ag [15], Zn [16] and non-metals such as N [17], C [18], S [19], and co-doping [20] is one of the most successful methods of overcoming this issue. TiO_2 nanoparticles could also be doped with tin to boost their photocatalytic capabilities. This metal can increase the number of hydroxyl radicals generated, which affects photocatalytic activity. Furthermore, using tin for doping is favorable due to the similar ionic structure of Sn^{4+} and Ti^{4+} particles (0.690 and 0.605, respectively), implying that Ti^{4+} can be replaced by Sn^{4+} in TiO_2 crystal structure [7]. Many researchers have studied the enhancement of photocatalytic activity after doping TiO_2 with Sn ions [7,10,12,13]. Rangel-Vázquez et al. (2015) used the sol-gel process using titanium and tin alkoxides to make Sn-doped TiO_2 with a band gap of 3.16 eV. They reported the presence of brookite phase in their samples in addition to anatase [7]. Arpac *et al.* (2007) prepared Sn-doped TiO_2 particles using a hydrothermal process. The resulting particles were thoroughly in the anatase phase with a purity of 84.09% [10]. In some recent studies, heating of TiO_2 nanoparticles in the presence of suitable metal salts has been used for doping various metals such as zinc, silver, copper, and iron [21,6-14,11]. Although the resulting doped nanoparticles had acceptable catalytic activity in the presence of visible light, however, higher activities are desirable for utilization in field applications. To the best of our knowledge, there are no reports focusing on the thermal doping of TiO_2 in the presence of tin salts. The thermal process would be much simpler, cheaper, and faster than other methods and would produce a high-purity product. Thus, we presented here a heat treatment method to prepare Sn-doped TiO_2 nanoparticles. In addition, the photocatalytic activity produced catalysts were examined for the degradation of methyl orange in aqueous solutions under visible lights, and the results were compared with the photocatalytic activity of pure anatase.

MATERIAL AND METHODS

All chemicals, including methyl orange, TiO_2 powder, and $SnCl_2$ were purchased from Merck Co.

Synthesis of Sn-doped TiO_2

Different amounts of $SnCl_2$ (3, 5, and 7 wt%) and TiO_2 were thoroughly mixed and blended. Each mixture was labeled regarding the containing amount of $SnCl_2$ (3%, 5%, and 7%). The mixture was heated in a 700 °C furnace for 60 minutes and then the resulting powder was completely washed with distilled water. The nanoparticles were then dried in an oven at 25 °C.

Characterization

LEO 1430VP instrument was used for scanning electron microscopy (SEM) and elemental dispersive X-ray spectroscopy (EDX) (LEO 1430VP, Germany). The powder X-ray diffraction analysis was done using a PW 1050 diffractometer (Philips, The Netherlands) with a Ni filter and Cu Kα (λ=1.54 Å) radiation. The average crystallite size of TiO_2 nanoparticles was calculated according to Scherrer's equation. A spectrophotometer was used to capture UV-Vis diffuse reflectance spectroscopy (DRS UV-Vis) in the wavelength range of 200–800 nm (Scinco S4100, S. Korea).

Photocatalytic activity

The photocatalytic activity of nanoparticles was investigated by the degradation of methyl orange. The amount of 50 ml solution with a concentration of 30 ppm was used for experiments. Firstly, nanoparticles (1 g catalyst/L solution) were added to methyl orange solution and stirred for 15 minutes in darkness. This was due to the stabilization of absorption and desorption between the organic dye molecules and the nanoparticles. Later on, the colloidal solution was settled under irradiation of a 90 W halogen lamp (Philips, Netherlands) at room temperature (Fig. 1). Subsequently, the photocatalyst solution was centrifuged and the degradation rate was immediately measured by a UV-visible spectrophotometer the rate was calculated using the following equation:

$$\text{Degradation efficiency (\%)} = \left(\frac{A_0 - A}{A_0}\right) \times 100 \qquad (1)$$

Where A_0 represents the initial absorption of the dye solution and A denotes the initial absorption after irradiation.

RESULTS AND DISCUSSION

Characterization

Fig. 2 is demonstrating SEM images of pure TiO_2 and sample 7%. The accumulated spherical-shaped particles of relatively the same size are seen in a pure sample (Fig. 2-a). As can be seen, this state is almost preserved in sample 7% (Fig. 2-b). Accordingly, it can be deduced that the used synthesis method has not had any significant

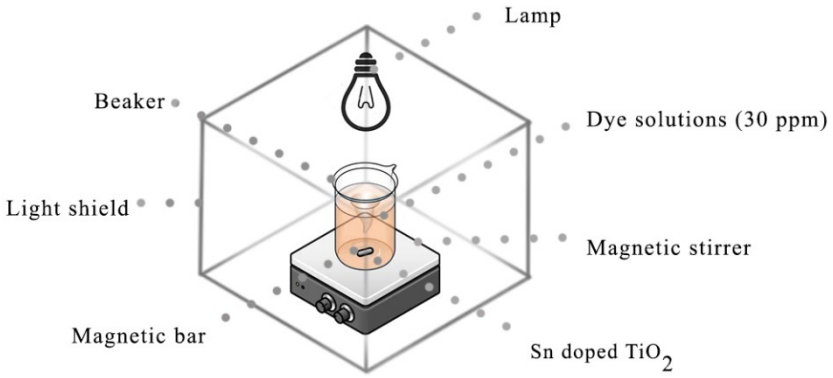

Fig. 1. Schematic diagram of photoreactor

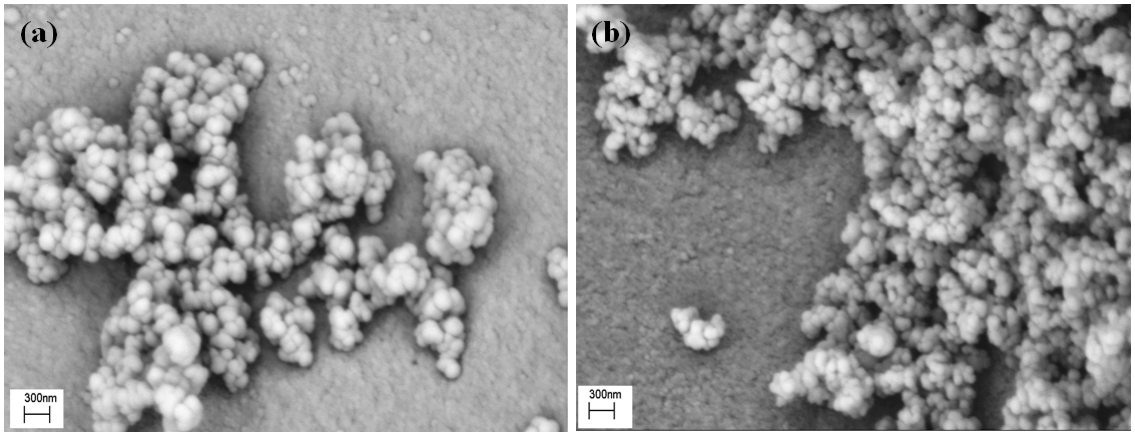

Fig. 2. The SEM images of a) pure TiO_2 nanoparticles and b) sample 7%.

effect on the morphology of TiO_2 nanoparticles. However, the sample 7% particles are smaller than TiO_2 particles with regards to size (Fig 1-B). A literature survey indicates that similar uniform and spherical-shaped morphologies have been reported in the case of iron-silver doped TiO_2 [4,14].

Fig. 3 shows the EDX spectra of prepared samples. Considering the chemical compositions, pure TiO_2 and Sn-doped TiO_2 compositions are given in Table 1. Given clear evidence, Sn-doped samples have experienced an increase in tin content. Moreover, the table reveals the presence of elemental Sn and TiO_2 compounds.

The XRD analysis was used to the advantage of crystalline phase observations. The results are given in Fige 4. It is proved that all the peaks which are around 25.8°, 37.4°, 48.9°, 54.7° and 55.9° present in XRD patterns of pure TiO_2 are consistent with anatase (1 0 1), (0 0 4), (2 0 0), (1 0 5) and (2 1 1) crystalline planes [14,21]. Like pure nanoparticles, samples 3, 5, and 7 only contain anatase peaks. Consequently, it could be said that the used doping method has no significant effect on the crystalline structure of TiO_2 nanoparticles. Also, there has been no evidence showing the presence of either rutile or brookite in the XRD patterns. This is in agreement with the results of studies on doping with iron, copper, and silver prepared in a similar way to this study [4,14]. Similarly, no pattern regarding the tin-related phase was witnessed. Sn ions were evenly distributed throughout the anatase crystallite of TiO_2, according to the predominant chemical state of Sn^{4+} [10]. On the other hand, the combined ion in the crystalline structure of TiO_2 was Sn^{4+}.

In Table 2, the crystalline sizes for anatase as a function of Sn^{4+} content are shown. It can be seen that, by increasing the amount of Sn^{4+}, there is a significant reduction in the crystallite size of the anatase from 9.2 nm for a pure sample to 5.8 nm

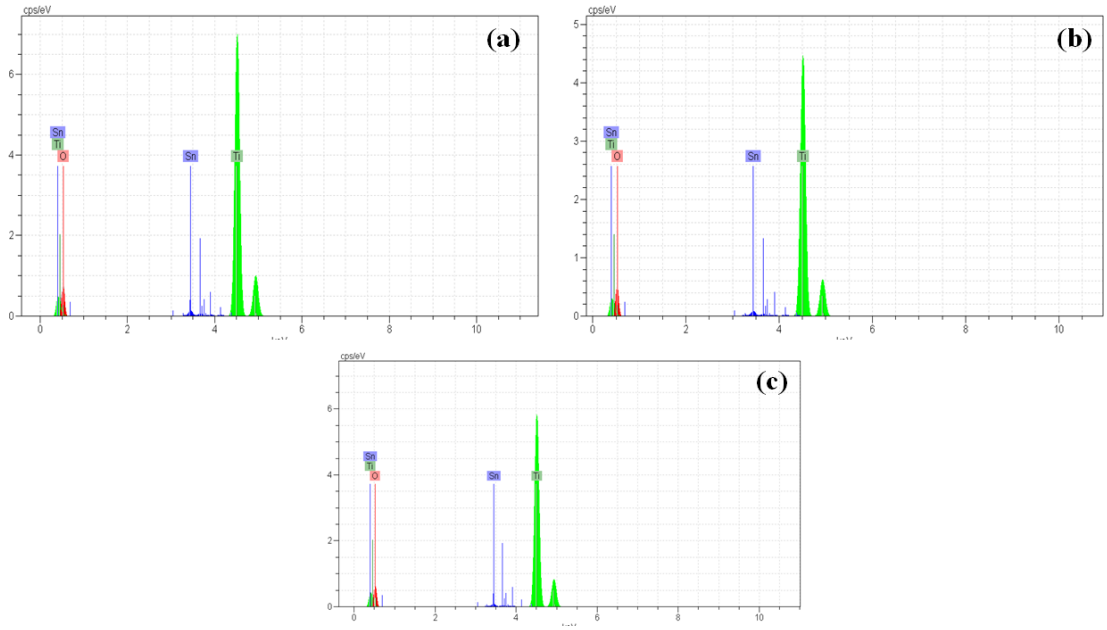

Fig. 3. The EDX spectra of a) sample 3%, b) sample 5% and c) sample 7%

Table 1. EDX analysis of pure and various Sn-doped TiO_2 nanoparticles

Element	Weight %			
	pure TiO_2	sample 3%	sample 5%	sample 7%
Oxygen	35.36	25.50	25.61	24.15
Titanium	64.64	73.14	72.55	73.75
Tin	0	1.37	1.84	2.10

for a sample of 7%. In a six-coordination, like that present in anatase structures, the ionic radii of Ti^{4+} and Sn^{4+} are 0.605 and 0.69 Å, respectively. This difference which is around 14% in size, should be introducing a perturbation in the crystal structure of anatase, in a way that inhibits the growth of the crystallites [7,10].

The absorption of UV-Visible irradiations for pure TiO_2 and Sn-doped nanoparticles is given in Figure 5. Photocatalytic absorption of visible light drastically increased after doping TiO_2 with Sn. A dramatic shift in the red light region (380-500 nm) is also observed. This can be attributed to the transitions called "charge transfer" between the titanium dioxide conduction band and Sn^{4+} doped electrons. As Sn-doped titanium dioxide photocatalytic activity is extended in the visible light region, there is a possible enhancement in this characteristic of TiO_2. The band gap energy of samples was calculated by using the equation: E_g (eV) = 1240/wavelength in nm [22]. E_g values for Sn-doped nanoparticles are 3.14, 2.70, 2.90, and 2.68 eV where the value is 3.2 eV for pure TiO_2. Notably, the addition of Sn has slightly modified the optical behaviors of the above-mentioned by shifting it towards the red region. The calculated band gap values are proved to be far less than similar studies [10, 13].

Photocatalytic performance

The photocatalytic activities of the as-prepared photocatalysts were evaluated by degrading methylene orange under visible light irradiation. The photocatalyst was added as 1 g catalyst/L

Table 2. Crystallite size of pure and Sn-doped TiO_2 nanoparticles

Sample	Crystal size (nm)
0	9.2
3%	7.7
5%	6.6
7%	5.8

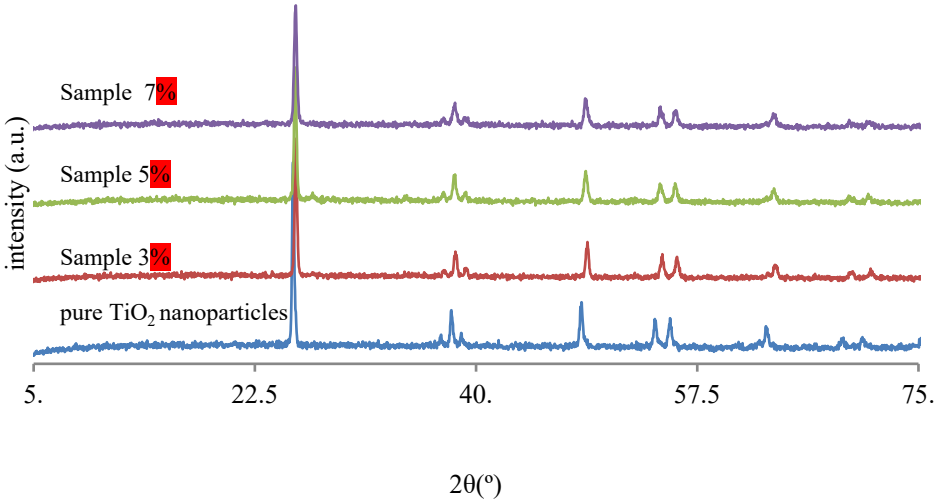

Fig. 4. XRD patterns of pure and Sn-doped TiO_2 nanoparticles

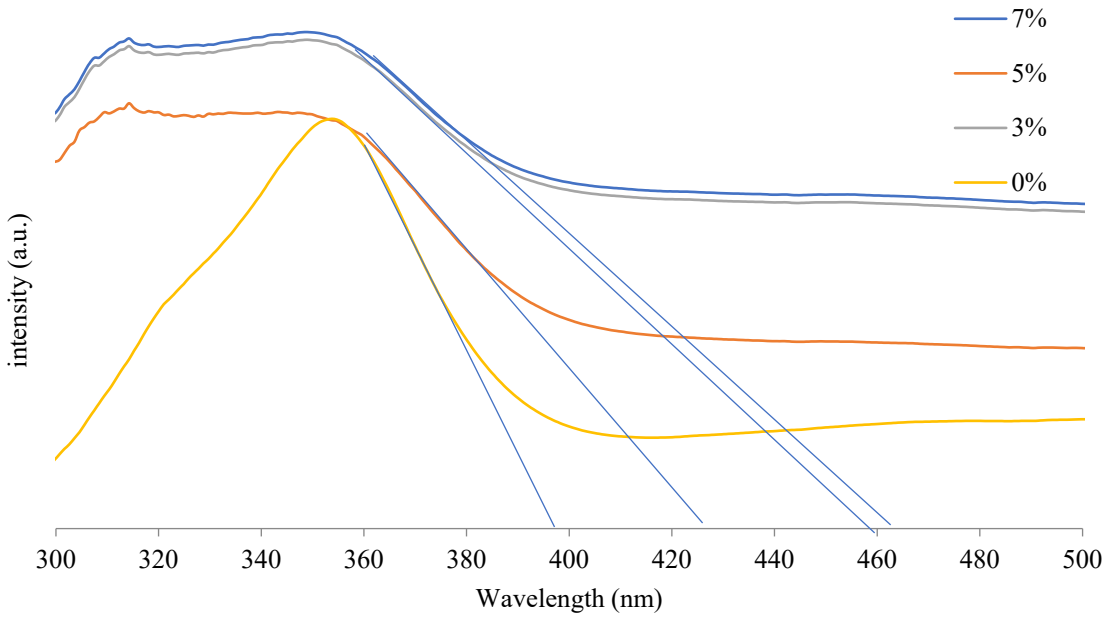

Fig. 5. UV–vis absorption spectra of pure and Sn-doped TiO_2 nanoparticles

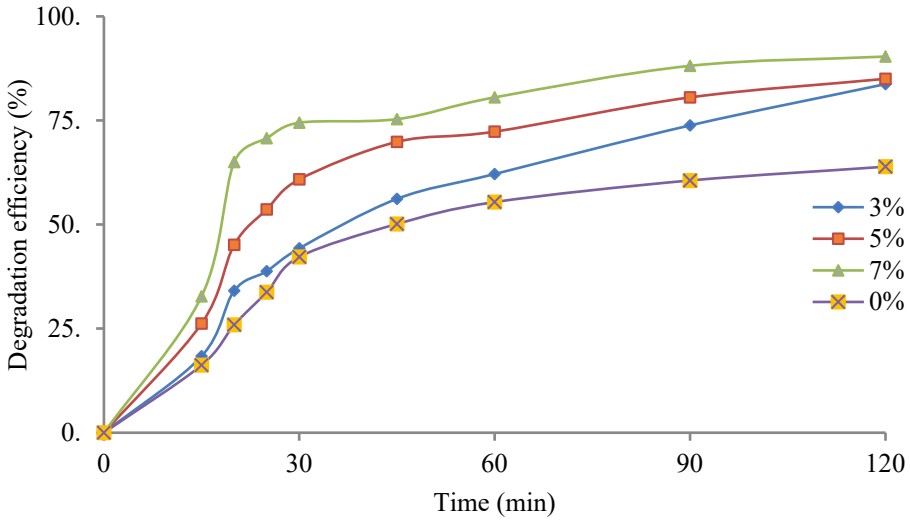

Fig. 6. The photocatalytic performance of pure and Sn-doped TiO_2 nanoparticles

solution. Figure 6 illustrates the degradation results; It is revealed that the photo-activity of Sn-doped nanoparticles is higher than pure TiO_2 under visible light irradiation. Degradation and photo-decolorization of methyl orange dye were determined after 120 minutes for each sample and values of 83%, 85%, and 90% were reported for samples 3%, 5%, and 7%. It is observed that the addition of Sn ions has enhanced the photo-activity of the nanoparticle.

There are various reasons for the increase in photocatalytic performance such as the smaller size of Sn-doped TiO_2 nanoparticles. On the other hand, the substitution of Sn^{4+} ions by Ti^{4+} ions in TiO_2 produces a distortion in the network which leads to structural defects on the surface, resulting in the presence of unsaturated surface cations and surface hydroxyl groups. The unsaturated sites favor the adsorption of the organic molecule on the surface defects of nanoparticles, where the molecule is oxidized by the photogenerated holes in the valence band. With the increase of the specific surface area in tin-doped- TiO_2 samples, an increase in the number of unsaturated sites and an enhancement in the photocatalytic activity should be expected. However, the activities of the sample 3% and 5% do not go far from that shown by the sample 7%. Furthermore, it was reported that Sn^{4+} incorporation leads to an increase in surface oxygen vacancies on TiO_2. However, high oxygen vacancies in samples 3% and 5% can act as recombination centers and inhibit photoactivity increment [7,10].

A comparison between the photocatalytic performance of the above nanoparticles and some other results reported for other metal-doped TiO_2 (which were produced using the same heat treatment method) revealed that the Sn-doped TiO_2 has higher efficiency and capability towards dye degradation [11,14]. For instance, it has been reported that Cu-doped TiO_2 nanoparticles could remove less than 80% of methyl orange at a dye concentration of 30 ppm [11]. The insufficient dye degradation was attributed to the phase transformation (Anatase → Rutile) and nanoparticle agglomeration during the doping treatment. Also, another study showed that the ability of Fe-doped TiO_2 nanoparticles in photocatalytic degradation of methyl orange at the concentration of 25 ppm was about 70%.

CONCLUSION

Pure TiO_2 and Sn-doped TiO_2 nanoparticles were produced by heating TiO_2 nanoparticles in the presence of $SnCl_2$ (3, 5, and 7 percent w/w) at 700 °C for 60 minutes. TiO_2 nanoparticles of both pure and Sn-doped TiO_2 are relatively spherical-shaped particles with relatively the same size. In both the pure and Sn-doped TiO_2 nanoparticles, the anatase was the only crystalline structure. By increasing the amount of dopant, there is a reduction in the crystallite size of the anatase from 9.2 nm for a pure sample to 5.8 nm for a sample of 7%. Photocatalytic absorption of visible light drastically increased after doping TiO_2 with Sn. After 120 minutes, the

degradation rates of samples 3%, 5%, and 7% that underwent methyl orange photo-decomposition were 85%, 85%, and 90%, respectively. The superior catalytic activities of the catalyst were attributed to the structural and consequently band gap changes in anatase by the incorporation of Sn ions into the TiO_2 lattice. Compared to pure TiO_2, which has a band gap of 3.2 eV, the band gap values for doped TiO_2 ranged from 3.14 to 2.68 eV. It was concluded that the produced Sn-doped TiO_2 nanoparticles are an efficient catalyst for methyl orange degradation. The proposed heat treatment method is fast and straightforward and can be used to control the anatase structure and maximize its dye removal capability.

CONFLICT OF INTEREST

The authors declare no conflict of interest.

REFERENCES

1. Buha, J., 2014. Optical properties and structure of the TiN-nitrogen-doped TiO2 nanocomposite. Applied surface science, 321: 457-463. https://doi.org/10.1016/j.apsusc.2014.10.039
2. Rzaij, J.M. and A.M. Abass, 2020. Review on: TiO2 thin film as a metal oxide gas sensor. Journal of Chemical Reviews, 2(2): 114-121. https://doi.org/10.33945/SAMI/JCR.2020.2.4
3. Amiri, M.R., M. Alavi, M. Taran, and D. Kahrizi, 2022. Antibacterial, antifungal, antiviral, and photocatalytic activities of TiO2 nanoparticles, nanocomposites, and bio-nanocomposites: Recent advances and challenges. Journal of Public Health Research, 11(2): 22799036221104151. https://doi.org/10.1177/22799036221104151
4. Madadi, M., M. Ghorbanpour, and A. Feizi, 2018. Antibacterial and photocatalytic activity of anatase phase Ag-doped TiO2 nanoparticles. Micro & Nano Letters, 13(11): 1590-1593. https://doi.org/10.1049/mnl.2018.5057
5. Cai, J., J. Shen, X. Zhang, Y.H. Ng, J. Huang, W. Guo, C. Lin and Y. Lai, 2019. Light-driven sustainable hydrogen production utilizing TiO2 nanostructures: a review. Small Methods, 3(1): 1800184. https://doi.org/10.1002/smtd.201800184
6. Padmanabhan, N.T., N. Thomas, J. Louis, D.T. Mathew, P. Ganguly, H. John and S.C. Pillai, ,2021. Graphene coupled TiO2 photocatalysts for environmental applications: A review. Chemosphere, 271: 129506. https://doi.org/10.1016/j.chemosphere.2020.129506
7. Rangel-Vázquez, I., G. Del Angel, V. Bertin, F. González, A. Vázquez-Zavala, A. Arrieta, J.M. Padilla, A. Barrera and E. Ramos-Ramirez, 2015. Synthesis and characterization of Sn doped TiO2 photocatalysts: Effect of Sn concentration on the textural properties and on the photocatalytic degradation of 2, 4-dichlorophenoxyacetic acid. Journal of Alloys and Compounds, 643: S144-S149. https://doi.org/10.1016/j.jallcom.2014.12.065
8. Ghahramani Jajin, R., A. Feizi, and M. Ghorbanpour, 2021. Reduction of Water Evaporation from Dam Reservoirs Using Hydrophobic Silver-Doped Titanium Dioxide Nanoparticles Coating. Water Resources Research, 57(5): p.e2020WR029231.9. Ghorbanpour M, Lotfiman S. Solid-state immobilisation of titanium dioxide nanoparticles onto nanoclay. Micro & Nano Letters. 2016; 11(11):684-7 https://doi.org/10.1049/mnl.2016.0259
10. Arpac, E., F. Sayılkan, M. Asiltürk, P. Tatar, N. Kiraz, and H. Sayılkan, 2007. Photocatalytic performance of Sn-doped and undoped TiO2 nanostructured thin films under UV and vis-lights. Journal of Hazardous Materials, 140(1-2): 69-74. https://doi.org/10.1016/j.jhazmat.2006.06.057
11. Madadi, M., M. Ghorbanpour, and A. Feizi, 2019. Preparation and characterization of solar light-induced rutile Cu-doped TiO2 photocatalyst by solid-state molten salt method. Desalination and Water Treatment, 145: 257-261. https://doi.org/10.5004/dwt.2019.23484
12. Sayılkan, F., M. Asiltürk P. Tatar, N. Kiraz, E. Arpac, and H. Sayılkan, 2007. Photocatalytic performance of Sn-doped TiO2 nanostructured mono and double layer thin films for Malachite Green dye degradation under UV and vis-lights. Journal of Hazardous Materials, 144(1-2): 140-146. https://doi.org/10.1016/j.jhazmat.2006.10.011
13. Koozegar Kaleji, B., S. Mirzaee, S. Ghahramani, S. Rezaie, N. Hosseinabadi, and A. Fujishima, 2018. Sol-gel synthesis of Sn/Fe co-doped TiO2 nanoparticles: study of structural, optical and photocatalytic properties. Journal of Materials Science: Materials in Electronics, 29(14):12351-12359. https://doi.org/10.1007/s10854-018-9348-x
14. Ghorbanpour M and A. Feizi, 2019. Iron-doped TiO2 Catalysts with Photocatalytic Activity. Journal of Water and Environmental Nanotechnology.4(1):60-6. https://doi.org/10.22090/jwent.2019.01.006
15. Ratshiedana, R., O.J. Fakayode, A.K. Mishra and A.T. Kuvarega, 2021. Visible-light photocatalytic degradation of tartrazine using hydrothermal synthesized Ag-doped TiO2 nanoparticles. Journal of Water Process Engineering, 44:102372. https://doi.org/10.1016/j.jwpe.2021.102372
16. Rajaramanan, T., S. Shanmugaratnam, V. Gurunanthanan, S. Yohi, D. Velauthapillai, P. Ravirajan, and M. Senthilnanthanan, 2021. Cost effective solvothermal method to synthesize Zn-doped TiO2 nanomaterials for photovoltaic and photocatalytic degradation applications. Catalysts, 11(6): 690. https://doi.org/10.3390/catal11060690
17. Huang, J., L. Dou, J. Li, J. Zhong, M. Li and T. Wang, 2021. Excellent visible light responsive photocatalytic behavior of N-doped TiO2 toward decontamination of organic pollutants. Journal of hazardous materials, 403: 123857. https://doi.org/10.1016/j.jhazmat.2020.123857
18. Pandi, K., M. Preeyanghaa, V. Vinesh, J. Madhavan and B. Neppolian, 2022. Complete photocatalytic degradation of tetracycline by carbon doped TiO2 supported with stable metal nitrate hydroxide. Environmental Research, 207: 112188. https://doi.org/10.1016/j.envres.2021.112188
19. Yu, H., M. Zhang, Y. Wang, J. Lv, Y. Liu, G. He, and Z. Sun, 2021. Low-temperature strategy for vapor phase hydrothermal synthesis of C\N\S-doped TiO2 nanorod arrays with enhanced photoelectrochemical and photocatalytic activity. Journal of Industrial and Engineering Chemistry, 98:130-139. https://doi.org/10.1016/j.jiec.2021.03.021
20. Qu, G., H.Wang, X. Li, T. Wang, Z. Zhang, D. Liang and H. Qiang, 2021. Enhanced removal of acid orange II from aqueous solution by V and N co-doping TiO2-MWCNTs/γ-Al2O3 composite photocatalyst induced by pulsed discharge plasma. Water Science and Technology, 83(2): 257-270. https://doi.org/10.2166/wst.2020.579
21. Ghorbanpour, M. and A. Feizi, 2020. Application of synthesizing tri-metallic Zn and Ag co-doped TiO2 nano-photocatalyst by a one-step synthesis technique in treating water pollutants. Desalination and Water Treatment, 200: 187-195. https://doi.org/10.5004/dwt.2020.26094
22. Sakthivel, T., Kumar, K.A., Ramanathan, R., Senthilselvan, J. and Jagannathan, K., 2017. Silver doped TiO2 nano crystallites for dye-sensitized solar cell (DSSC) applications. Materials Research Express, 4(12): 126310. https://doi.org/10.1088/2053-1591/aa9e36